Atyaf S.F. Alrubaie

Branch of Basic Sciences, College of Dentistry, AL-Qadisiyah University, AL-Qadisiyah, IRAQ

Preparation and Characterization of Copper Nanoparticles by Pulsed-Laser Deposition

In this work nanostructured copper thin films were deposited on glass and silicon substrates by the pulsed-laser deposition (PLD) technique utilizing a Nd:YAG laser operating with a pulse energy of 480mJ, a repetition frequency of 6Hz, and 500 pulses. The results of characterizations showed clear peaks that indicated plasmonic absorption at a wavelength of 220nm. The predominance of the anatase Cu phase was revealed. The presence of spherical particles that were dispersed in clusters were also revealed. The average size of these clusters ranged from 66.2 to 90.7 nanometers.

Keywords: Nanoparticles; Copper; Pulsed-laser deposition; Structural characterization
Received: 06 January 2024; **Revised:** 29 February 2024; **Accepted:** 07 March 2024

1. Introduction

There has been an increasing fascination with creating and designing metal nanoparticles that have well-defined structures. This is because these materials possess distinct and auspicious characteristics. Copper (Cu) is a metal that has attracted considerable interest at the nanoscale. It is a versatile metal that finds extensive usage in electrical conductivity, catalysis, and antibacterial applications. Copper nanoparticles have distinctive optical characteristics, such as adjustable bandgaps and effective light absorption [1]. Copper (Cu) is a highly regarded metal known for its excellent qualities, which make it indispensable in numerous sectors. Substantial research and utilization of its unusual mix of physical, chemical, electrical, and thermal properties have been observed in varied domains [2]. Copper is highly recognized for its exceptional electrical conductivity. It possesses the most significant electrical conductivity compared to other commonly found metals, except superconductors at extremely low temperatures. Copper's characteristic of facilitating efficient current flow with minimal energy loss makes it a highly suitable material for electrical wiring, power transmission, and electronics. Copper also demonstrates exceptional heat conductivity. Due to its remarkable thermal conductivity, it is highly favored as a material for heat sinks, cooling systems, and heat exchangers. Its exceptional thermal conductivity facilitates efficient heat dissipation, making it indispensable for electronics, power generation, and thermal management. Copper exhibits superior ductility, malleability, and excellent electrical and thermal conductivity. It has excellent malleability, allowing it to be easily manipulated and molded into intricate shapes without any breaking risk, making it appropriate for manufacturing techniques, including rolling, extrusion, and forging. These characteristics facilitate the manufacturing complex copper parts used in plumbing, architecture, and industrial machinery. Nanotechnology is an interdisciplinary domain that includes scientific and technological endeavors focused on manipulating and regulating matter at the nanoscale, typically ranging from 1 to 100 nm in size. It encompasses the comprehension, creation, and production of materials, technologies, and systems having unique features and functionalities at a minuscule scale. At the nanoscale, the characteristics of materials can vary considerably compared to their larger forms. Nanotechnology harnesses these distinctive characteristics to create novel materials, devices, and procedures that find utility in diverse domains such as electronics, medicine, energy, materials research, and environmental science [2,3].

Copper exhibits excellent corrosion resistance, especially in both air and aquatic conditions. The metal develops a patina, a protective oxide layer on its surface that effectively inhibits additional corrosion. Copper's exceptional corrosion resistance makes it suitable for outdoor applications, architectural structures, and plumbing systems. In addition, copper demonstrates antibacterial capabilities, referred to as the "oligodynamic effect." Studies have shown that it possesses inherent antibacterial properties, which make it valuable for usage in healthcare facilities, antimicrobial coatings, and water purification systems [3].

2. Experimental Part

Copper exhibits exceptional electrical conductivity, second only to silver. Its efficient conductivity makes it popular for electrical wiring, power transmission, and electronics. Copper's exceptional thermal conductivity makes it an optimal selection for heat transfer applications. It is frequently employed in heat sinks, heat exchangers, and cooling systems. Copper exhibits exceptional ductility and malleability, allowing it to undergo extensive

elongation into wires or be effortlessly molded into diverse shapes without experiencing fracture. This feature enables the fabrication of complicated copper components using techniques such as rolling, drawing, and forging. Copper exhibits excellent corrosion resistance, especially in both air and aquatic conditions. The metal develops a defensive oxide layer, known as patina, on its surface, inhibiting additional corrosion. Its characteristics render it appropriate for use in outdoor applications and plumbing systems. Copper has natural antibacterial capabilities, referred to as the "oligodynamic effect." It demonstrates the capacity to eradicate or impede the proliferation of bacteria, viruses, and fungi on its surface. Copper's inherent characteristics have resulted in its use in healthcare environments, antimicrobial coatings, and water purification systems.

The pulsed-laser deposition (PLD) system schematically shown in Fig. (1) has been used to deposit thin films on different substrates. This system comprises the following components: a laser device, a deposition chamber, a rotary vacuum pump, a vacuum pressure monitoring device, a target holder, and an electronic thermometer. A Diamond-288 Pattern EPS Nd:YAG laser used was supplied by Huafei Tongda Technology. The laser energy may reach to 1900 mJ at wavelength of 1064nm, and the operation frequency ranges from 1 to 6 Hz. The pulse duration is 10ns. The laser system was water-cooled by flowing cool water to replace the heated water as a result of laser operation. This system also contains the deposition chamber made from Pyrex glass with a height of 30 cm, a diameter of 20 cm, and a thickness of 5 mm. The chamber is mounted on an aluminum base with a diameter of 30 centimeters and a thickness of 20 mm. A circular groove, measuring 2 cm in width and 5 mm in depth, was formed on the upper surface of this base. An O-ring is placed inside this groove to prevent the leak of the deposition chamber. The vacuum of 10^{-3} mbar inside the deposition chamber was created by using a rotary vacuum pump (Varian Rotary Pump DC 302 949-9325 s 006 W/Leroy L 080 BR type). To reach 10^{-6} mbar vacuum level, a diffusion pump supplied by Mancha Vacuum Technologies was used.

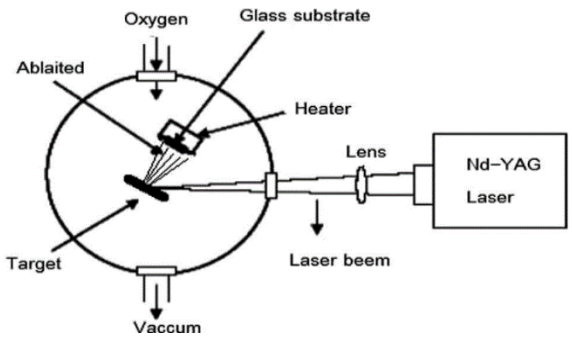

Fig. (1) Scheme of the PLD system used in this work

The target holder is made from stainless steel with a diameter of 2 cm and a depth of 3 mm. A tiny rotary motor was employed to rotate the holder at a speed of 10 r.p.m. The rotation of the holder is done consistently to ensure that the laser energy is evenly distributed on the compressed material (target), resulting in a uniform deposition of prepared films. The temperature of elements inside the chamber was monitored using a thermocouple. Precise measurement of the substrate temperature is crucial in thin film growth. A 250W halogen lamp was used to warm the substrate up to 400°C.

The system's interior was cleaned with alcohol to prevent the contamination by any residue from previously deposited substances. The material to be deposited is placed in a tungsten boat, which has a high melting point that is significantly higher than the melting point of the material to be deposited. The substance being used is pure copper. The boat is linked to a pair of electrodes connected to an internal electric current source within the system to be electrically heated. As the substance melts, we gradually raise the electric current provided to the electrodes, therefore, the material undergoes a process of glowing, which involves the evaporation of the material and the deposition of a film on the substrate. Once the material is entirely deposited, the current is gradually decreased. The sample oxidation is prevented because the system is left for 30 minutes after the deposition process is completed. The copper film deposition process includes the following stages:

- The interaction between the laser beam and the copper target
- The generation and enlargement of plasma within the deposition chamber, directed towards the glass slide where the deposition occurs, is induced by laser beams. The film was deposited onto a glass substrate (slide) at room temperature and under 10^{-3} mbar vacuum pressure. The laser energy was 600 mJ, with a frequency of 6 Hz. The incident laser beam was directed at an angle of 45° to the target surface, and the slide was positioned 10 cm above the target.

The film thickness (t) was determined by the weight method as follows:

$$t = \frac{M}{\pi \rho L^2} \qquad (1)$$

where M is the mass of the substance (g), ρ is the density of the substance (g/cm^3), and L is the distance between the crucible and the substrate stand (cm)

The structure, surface morphology, and optical properties of the deposited films were determined by x-ray diffraction (XRD), field-emission scanning electron microscopy (FE-SEM), energy-dispersive x-ray spectroscopy (EDX), and UV-visible spectrophotmetry.

3. Results and Discussion

The x-ray diffraction used for the diagnosis of structure of the prepared films is based on Bragg's law to determine the inter-planar distance (d_{hkl}) as [10]

$$n\lambda=2d_{hkl}\,sin\theta \quad (2)$$

where n represents the diffraction order, θ represents the diffraction angle, and λ is the x-ray wavelength, which is pertained by the metal target used to produce the x-ray radiation

The Scherrer's formula shown below was used to determine the crystallite size, which is inversely proportional to the full-width at half maximum (FWHM) of diffraction peaks [11]:

$$C.S=\frac{0.9\,\lambda}{\beta.cos\theta} \quad (3)$$

where β is the FWHM

The XRD pattern of the prepared nanoparticles is depicted in Fig. (2). It displays diffraction peaks at 2θ of 27.34°, 29.99°, 31.89°, 35.69°, 39.89°, 45.59°, and 53.14°, which are assigned to crystal planes of (111), (110), (200), (210), (211), (220), and (311), respectively, belonging to the crystal structure of copper. The presence of these peaks confirms the formation of nanomaterial with a high degree of crystallinity. Also, the Cu nanoparticles can be inferred to be in the anatase phase, as indicated by the Joint Committee on Powder Diffraction Standard (JCPDS) (card no. 00-0333-0492).

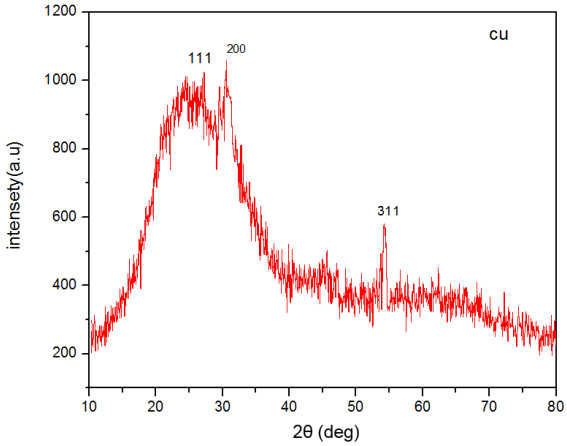

Fig. (2) XRD pattern of Cu NPs prepared in this work by PLD

The diffraction peaks of the processed samples exhibit distinct domain peaks at (111), (200), and (311) orientations, occurring at approximately 2θ = 27.34°, 31.89º, and 53.14°, respectively, ascribed to a cubic structure of Cu anatase phase with lattice constants a=b=c=3.615nm and angles α=β=γ=90°. The XRD pattern does not show peaks of other materials, indicating the samples were prepared with high purity, as illustrated in table (1). It was observed that there were minor variations in the match due to a slight increase in thickness, contaminants, or voids in the film. The granularity level is directly proportional to the thickness and inversely proportional to the width of the center peak observed in XRD pattern [12,13].

The absorption spectrum of Cu nanoparticles prepared using laser energy of 480mJ is shown in Fig. (3). It shows that the absorbance is high within the range of 190-300nm, with a prominent peak at 220nm. The transmittance of Cu nanoparticles shown in Fig. (4) reaches its minimum at the same wavelength. The absorbance decreases at wavelengths longer than 220nm. The appearance of these peaks can be attributed to the quantum size effect. The plasmon peaks' intensity and width were shown to depend on both laser energy and the number of laser pulses. The aggregation of the prepared Cu nanoparticles within a few days, which agrees with the observations of Anikin et al. [14].

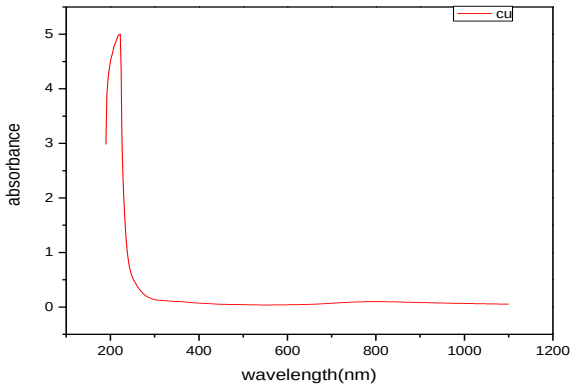

Fig. (3) UV-visible absorption spectrum of of Cu NPs prepared in this work by PLD

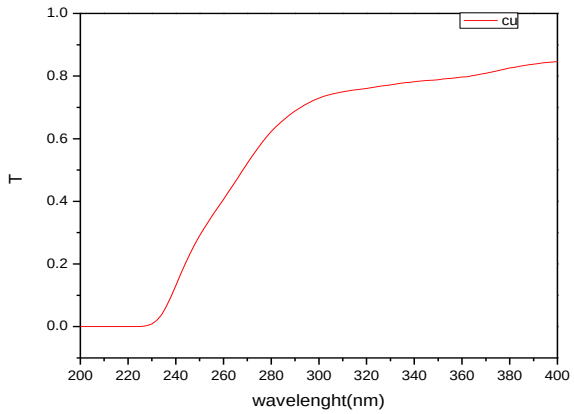

Fig. (4) UV-visible transmission spectrum of Cu NPs prepared in this work by PLD

The surface morphology of the produced samples was examined using FE-SEM, as depicted in Fig. (5). The FE-SEM image reveals that the sample prepared using 480 mJ laser energy have a nanostructure characterized by a distribution of spherical particles. The spherical clusters are spread in various places with an average diameter of 7.72 nm, as indicated in table (2). It was observed that the sample had a rough surface and large pore size, resulting in a high specific surface area.

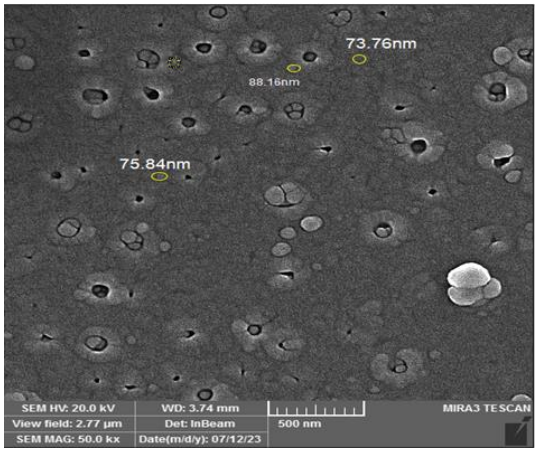

Fig. (5) FE-SEM image of Cu NPs prepared in this work by PLD

Table (2) FE-SEM results of of of Cu NPs prepared in this work by PLD

Label (Cu)	Area	Particle Size (nm)		
		Mean	Min	Max
1	0.016	88.167	43.000	141.000
2	0.019	73.769	40.000	109.000
3	0.019	73.769	40.000	109.000
4	0.018	75.844	28.000	120.000
5	0.006	73.344	49.000	100.000
6	0.011	82.083	41.000	121.000
7	0.006	66.656	42.000	109.000
8	0.016	76.841	47.000	114.000
9	0.018	70.742	38.000	115.000
10	0.016	92.333	44.000	146.000

4. Conclusion

The study showed the one-step preparation process of spherical-shaped copper nanoparticles using PLD technique. The prepared Cu nanoparticles have a single-phase cubic structure (anatase Cu). The laser fluence determines the form and size of the nanoparticles. The presence of extensively clustered Cu particles measuring 41–77 nm was verfieid depending on the laser fluence.

References

[1] J.D. Smith and A.B. Johnson, "Selection of Copper (Cu), Cadmium Sulfide (CdS), Zinc (Zn), and Tin (Sn) for Nanomaterial Fabrication: Characteristics and Applications", *J. Adv. Mater.*, 10(2) (2022) 45-60.

[2] Y. Huang et al., "Decorated Cu NPs on Lignin Coated magnetic Nanoparticles: Its Performance in The reduction of Nitroarenes and Investigation of Its Anticancer Activity in A549 Lung Cancer Cells", *Arabian J. Chem.*, 14 (2021) 103299.

[3] R. Hultgren and P.D. Desai, "Selected Thermodynamic Values and Phase Diagrams for Copper and Some of Its Binary Alloys, Incra Monograph I", International Copper Research Association Inc. (NY, 1971).

[4] C.T. Avedisian et al., "Nanoparticles for Cancer Treatment: Role of Heat Transfer", *Annals New York Acad. Sci.*, 1161(1) (2009) 62–73.

[5] R.K. Swarnkar, S.C. Singh and R. Gopal, "Effect of Aging on Copper Nanoparticles Synthesized by Pulsed Laser Ablation in Water: Structural and Optical Characterizations", *Bull. Mater. Sci.*, 34(7) (2011) 1363-1369.

[6] A.V. Simakin et al., "Nanoparticles Produced by Laser ablation of Solids in Liquid Environment", *Appl. Phys. A: Mater. Sci. Process.*, 79 (2004) 1127-1132.

[7] D.M. Mattox, **"Handbook of Physical Vapor Deposition (PVD) Processing: Film Formation, Adhesion, Surface"**, William Andrew Inc. (NY, 1998).

[8] T. Ctvrtnickova et al., "Laser Deposition of Powdered Samples and Analysis by Means of Laser-Induced Breakdown Spectroscopy", *Appl. Surf. Sci.*, 255 (2009) 5329-5333.

[9] M. Kim et al., "Synthesis of Nanoparticles by Laser Ablation", *KONA Powder Particle J.*, 34 (2017) 80–90.

[10] R. Herrero-Vanrell et al., "Self-assembled Particles of an elastin-like polymer as vehicles for controlled drug release", *J. Control. Rel.*, 102 (2005) 113–122.

[11] R.L. Siegel, K.D. Miller and A. Jemal, "Cancer statistics", *CA Cancer J. Clin.*, 70 (2020) 7–30.

[12] A.H.O. Alkhayatt et al., "Characterization of CuO/n–Si pn junction synthesized by successive ionic layer adsorption and reaction method", *Opt. Quantum Electron.*, 51(7) (2019) 233.

[13] L. Madler et al., "Controlled synthesis of nanos-tructured particles by flame spray pyrolysis", *J. Aerosol. Sci.*, 33(2) (2002) 369–389.

[14] K. Anikin et al., "Formation of ZnSe and CdS quantum dots via laser ablation in liquids", *Chem. Phys. Lett.*, 366(3-4) (2002) 357-360.

Table (1) XRD results for the Cu nanoparticles prepared by pulsed-laser deposition

Sample	2θ (deg) standard	2θ (deg) Observed	d(Å) Standard	d(Å) Observed	(hkl)	Standard Card
Cu	27.4202	27.3442	3.2500	3.2422	(111)	00-0333-0492
	29.9808	29.9940	2.9780	2.9848	(110)	00-034-1354
	31.8193	31.8940	2.8100	2.8688	(200)	00-0333-0492
	35.4512	35.694	2.5300	2.5881	(210)	00-0333-0492
	39.1866	39.8940	2.2970	2.8865	(211)	00-0333-0492
	45.4729	45.5940	1.9930	1.6518	(220)	00-0333-0492

